



Unique roles of aminophospholipid translocase Drs2p in governing efflux pump activity, ergosterol level, virulence traits, and host–pathogen interaction in *Candida albicans*

Shweta Singh¹ · Sandeep Hans¹ · Aijaz Ahmad^{2,3} · Zeeshan Fatima¹ · Saif Hameed¹

Received: 4 April 2022 / Revised: 3 June 2022 / Accepted: 22 June 2022 / Published online: 5 July 2022
© The Author(s), under exclusive licence to Springer Nature Switzerland AG 2022

Abstract

Infections caused by *Candida albicans* are rising due to increment in drug resistance and a limited arsenal of conventional antifungal drugs. Thus, elucidating the novel antifungal targets still represent an alternative that could overcome the problem of multidrug resistance (MDR). In this study, we have uncovered the distinctive effect of aminophospholipid translocase (Drs2p) deletion on major MDR mechanisms of *C. albicans*. We determined that efflux activity was diminished in $\Delta drs2$ mutant as revealed by extracellular rhodamine 6G (R6G) efflux and flow cytometry. Moreover, we further unveiled that $\Delta drs2$ mutant displayed decreased ergosterol content and increased membrane fluidity. Furthermore, Drs2p deletion affects the virulence attributes and led to inhibited hyphal growth and reduced biofilm formation. Additionally, THP-1 cell lines' mediated host–pathogen interaction studies revealed that $\Delta drs2$ mutant displayed enhanced phagocytosis and altered cytokine production leading to increased IL-6 and decreased IL-10 production. Taken together, the present study demonstrates the relevance of Drs2p in *C. albicans* and consequently disrupting pathways known for mediating drug resistance and immune recognition. Comprehensive studies are further required to authenticate Drs2p as a novel antifungal drug target.

Keywords *Candida albicans* · Flippase · Drs2p · Aminophospholipid translocase · Efflux pump · Ergosterol · Virulence trait · Host–pathogen interaction

Introduction

Candida albicans is a dimorphic human fungal pathogen that causes mucosal and systemic infections in immunocompromised individuals and affects many populations (Ravikant Kaur et al. 2015; Singh et al. 2015; Arendrup and Patterson 2017; Bongomin et al. 2017, CDC reports 2019). Multidrug resistance (MDR) is a major impediment against the present

armamentarium of antifungal drugs towards their limited and restricted usage (Robbins et al. 2016). There are different mechanisms of MDR that are well documented such as overexpression of efflux pumps, alteration of drug target (ergosterol content), and elevated chitin content that has been mainly implicated in azole and echinocandin resistance, respectively (Tanwar et al. 2014; Pristov and Ghannoum 2019). Moreover, *Candida* forms biofilm which is recalcitrant to a wide spectrum of antifungal drugs (Zarnowski et al. 2018). This urges the need to either develop new antifungal agents or identify novel targets unique to fungi. The development of new antifungal agents is a time-consuming process where many hurdles such as toxicities, drug interactions, and difficulties in intravenous administration need to be worked (Wiederhold 2018). Alternatively, it would be better to indulge in studies that aids in the recognition of novel antifungal targets that are unique and specific for pathogens including *C. albicans*. The recent understanding and advancements in techniques have allowed for the identification of potential new targets that can strengthen the resources of understanding *Candida* resistance.

✉ Zeeshan Fatima
drzeeshanfatima@gmail.com

✉ Saif Hameed
saifhameed@yahoo.co.in

¹ Amity Institute of Biotechnology, Amity University Haryana, Gurugram (Manesar) 122413, India

² Clinical Microbiology and Infectious Diseases, School of Pathology, Faculty of Health Sciences, University of the Witwatersrand, Johannesburg 2193, South Africa

³ Infection Control, Charlotte Maxeke Johannesburg Academic Hospital, National Health Laboratory Service, Johannesburg 2193, South Africa

The cell membrane is known to play a crucial role in fungal growth as it acts as a barrier that mediates the transport of nutrients, maintains osmolarity, pH sensing, and regulates defense against any environmental insults. The multifunctionality of the cell membrane makes it one of the most common drug targets of antifungal drugs (Douglas and Konopka 2016). The complex functionality of cell membrane is due to array of different proteins and lipids present in the membrane. In *C. albicans*, the physical properties of the membrane and lipid functions have close relation to MDR development. For instance, membrane lipid phase and asymmetry affect azole resistance (Kohli et al. 2002). Similarly, drug diffusion and the membrane lipid environment also regulate the drug susceptibility phenotype of *Candida* (Pasrija et al. 2005; Prasad et al. 2005). The susceptibility of *Candida* cells to antifungal drugs is also governed by ergosterol and sphingolipid content as the knockout mutants of ergosterol and sphingolipid biosynthetic pathways were susceptible to antifungal drugs such as azoles in comparison to their wild-type strains (Mukhopadhyay et al. 2004; Pasrija et al. 2008). Thus, the role of membrane lipid homeostasis in governing MDR is evident from wide range of studies.

Lipid asymmetry is vital for many cellular functions such as the budding of vesicles and membrane curvature (Oliveira et al. 2013). P-type ATPases are the ATP-dependent family of transporters that are involved in the transport of heavy metals and ions. However, some members like the P4 type, instead of being cation transporters, are proposed to be aminophospholipid translocase of flippase that translocate the phosphatidylserine (PS) and phosphatidylethanolamine (PE) from outer leaflet to inner leaflet membrane bilayer. Drs2p is a P4-type ATPase essential for the flippase activity of PS in the trans-Golgi network in yeast cells with no human homologue (Hua et al. 2002; Sebastian et al. 2012). It is known that Drs2p governs PE asymmetry in post-Golgi secretory vesicles (Natarajan et al. 2004; Zhou and Graham 2009). Drs2p functions by utilizing the energy from hydrolysis of ATP for translocation of PS and PE across the membrane. The non-catalytic unit of flippase known as Cdc50 has been studied in *C. albicans* and is known to govern antifungal drug resistance, virulence, hyphal development, and endocytosis (Xu et al. 2019). The role of P-type ATPases in

regulating virulence factors has also been demonstrated in another fungal pathogen such as *Cryptococcus neoformans* (Huang et al. 2016).

The aim of the present study is to strengthen the available literature and elucidate the effect of Drs2p deletion in *C. albicans* on major MDR development mechanisms, virulence traits, and host–pathogen interaction. We explored that Drs2p functionality is indispensable for coordinated functioning in *C. albicans* as revealed by abrogated efflux pump activity, lower ergosterol content, inhibited hyphal development, and biofilm formation along with enhanced phagocytosis and altered cytokine production. This study supports the utility of Drs2p in governing drug resistance mechanisms and immune recognition that could be exploited for therapeutics.

Material and methods

All media and chemicals such as YPD (yeast extract peptone dextrose), agar, thiazolyl blue tetrazolium bromide (MTT), rhodamine 6G (R6G), dinitrophenol (DNP), 2-deoxy glucose (2-DOG), and serum were purchased from HiMedia (Mumbai, India). D-glucose and mannitol were obtained from Fischer Scientific. Crystal violet (CV), phorbol myristate acetate (PMA), and *n*-heptane were obtained from Sigma Chemical Co. (St. Louis, MO, USA).

Growth media and strains

The *Candida* strains (BWP17 and Δ drs2 mutant listed in Table 1) were used in this study and were kindly provided by Martine Bassilana group (Labbaoui et al. 2017). Δ drs2 mutant is derived from parent (WT) strain BWP17 and generated by homologous recombination. Each copy was replaced by either HIS1 or URA3, using knockout cassettes generated by amplification of pGemHIS1 and pGemURA3 with primer pairs DRS2.P1/DRS2.P2. Strains were cultured in YPD broth with the composition of yeast extract 1% (w/v), peptone 2% (w/v), and dextrose 2% (w/v). For agar plates, 2% (w/v) agar was added to the media. The cells were freshly revived on YPD agar plates and grown at 30 °C before each study to ensure the revival of the strains (Fig. S1).

Table 1 List of *C. albicans* strains used in this study

Name	Strain	Genome	Reference
4861	BWP17	ura3 Δ :: λ imm434/ura3 Δ :: λ imm434 his1 Δ ::hisG/his1 Δ ::his arg4::hisG/arg4 Δ ::hisG	Wilson et al. (1999)
PY3375	Δ drs2	ura3 Δ :: λ imm434/ura3 Δ :: λ imm434 his1 Δ ::hisG/his1 Δ ::his arg4::hisG/arg4 Δ ::hisG drs2 Δ ::HIS1/ drs2 Δ ::URA3 RP10::ARG4	Labboiu et al. (2017)

R6G extracellular efflux assay

The efflux of R6G was determined essentially using a previously described protocol (Singh et al. 2018). Briefly, approximately 1×10^6 yeast cells (WT and $\Delta drs2$ mutant) from an overnight-grown culture were transferred to a YPD medium and allowed to grow overnight. Cells were pelleted, washed twice with phosphate-buffered saline (PBS) (without glucose), and resuspended as a 2% cell suspension, corresponding to 10^8 cells (wt/vol) in PBS without glucose. The cells were then de-energized for 45 min in 2-DOG (5 mM) and 2,4 DNP (5 mM) in PBS (without glucose). The de-energized cells were pelleted, washed, and resuspended as a 2% cell suspension (w/v) in PBS without glucose, to which R6G was added at a final concentration of 10 μ M and incubated for 40 min at 30 °C. The equilibrated cells with R6G were then washed and resuspended as a 2% cell suspension (w/v) in PBS without glucose. Samples with a volume of 1 ml were withdrawn at the indicated time and centrifuged at $2500 \times g$ for 2 min. The supernatant was collected, and OD was measured at 527 nm. Energy-dependent efflux (at the indicated time) was measured after the addition of glucose (2%) to the cells resuspended in PBS (without glucose). Glucose-free controls were included in all the experiments. For the flow cytometric analysis of R6G extrusion, the abovementioned protocol was followed and R6G (10 μ M) was added before the final incubation of 40 min. The equilibrated cells with R6G were then washed and resuspended as a 2% cell suspension (w/v) in PBS without glucose. Samples with a volume of 1 ml were withdrawn at the indicated time and centrifuged at $2500 \times g$ for 2 min. The supernatants were discarded, and cells were taken for flow cytometry analysis. R6G accumulation was measured by evaluating the MFI of R6G in WT and $\Delta drs2$ mutant strains. The data were analyzed on BD FACS (USA) using Suite software.

Quantitation of ergosterol

Sterols were extracted by the alcoholic KOH method, and the percentage of ergosterol was calculated as described previously (Singh et al. 2016a, b). Briefly, single *C. albicans* colonies from an overnight YPD agar plate culture of WT and $\Delta drs2$ mutant were used to inoculate 50 ml of YPD. Both ergosterol and 24(28)DHE absorb at 285 nm, whereas only 24(28)DHE absorbs at OD_{230} nm. Ergosterol content was determined by subtracting the amount of 24(28)DHE (calculated from OD_{230}) from the total ergosterol plus 24(28)DHE content (calculated from $OD_{281.5}$). Ergosterol content was calculated as a percentage of the wet weight of the cells with the following equations:

$$\% \text{Ergosterol} + \% 24(28)\text{DHE} = \frac{\left[\left(\frac{A_{281.5}}{290} \right) \times F \right]}{\text{Pellet weight}}$$

$$\% 24(28)\text{DHE} = \frac{\left[\left(\frac{A_{230}}{518} \right) \times F \right]}{\text{Pellet weight}}$$

$$\% \text{Ergosterol} = [\% \text{Ergosterol} + \% 24(28)\text{DHE}] - [\% 24(28)$$

where F is the factor for dilution in petroleum ether and 290 and 518 are the E values (in percent per centimeter) determined for crystalline ergosterol and 24(28)DHE, respectively.

Membrane fluidity

To investigate the fluidity of the plasma membrane in WT and $\Delta drs2$ mutant, a fluorescent compound 1,6-diphenyl-1,3,5-hexatriene (DPH) was used in the study. It binds to the membrane lipid acyl groups when it is intercalated into lipid membranes emitting fluorescence. The cells incubated were harvested and resuspended in PBS. Then, the cells were fixed with 37% formaldehyde and washed thrice with cold PBS. Subsequently, the cells were frozen, thawed, incubated with 6 mmol DPH at 28 °C for 45 min, and washed thrice with PBS. The intensity of DPH fluorescence was analyzed using a spectrofluorometer (Agilent Technology, USA) at excitation and emission wavelengths of 350 and 425 nm, respectively (Fatima and Hameed 2020; Singh et al. 2020).

Yeast to hyphal transition

Yeast to hyphal induction for *C. albicans* was carried out on hyphal induction media such as serum (10% v/v serum in YPD), Spider, and SLAD. The dimorphic switching was performed using the protocol described elsewhere (Singh et al. 2016a, b). Briefly, the WT and $\Delta drs2$ mutant culture were grown overnight at 30 °C in YPD broth before each study. The revived cells were harvested by centrifugation at $5000 \times g$ for 3 min and washed twice and incubated at 37 °C for 6 h with PBS without glucose to induce starvation. After incubation, the cells were transferred to the required media for hyphal growth, and hyphae were observed under the light microscope at magnification of $40 \times$ and $4 \times$ for liquid and solid media, respectively.

Biofilm formation

The formation of biofilm in WT and $\Delta drs2$ mutant was assessed by the method described elsewhere (Singh et al. 2016a, 2016b). *Candida* biofilms were checked on the

polystyrene surface of 96-well plates. *Candida* cell suspension was prepared of 1×10^7 cells/ml in PBS, and 100 μ l of cells was seeded in each well of 96-well plate and incubated for 90 min at 37 °C with shaking. After incubation, the non-adhered cells were removed by gentle washing with PBS. Fresh 200 μ l YPD media were added to adhered cells in each well for 24 h at 37 °C. The cells were washed for biofilm visualization and stained with CV (0.05% w/v) in the wells and kept for 1 min. The extra stain was removed by washing with PBS, and stained biofilm was observed under the light microscope at 40 \times magnification.

For quantification of biofilm formed in wells of 96-well plate, tetrazolium salt 3-[4,5-dimethylthiazol-2-yl]-2,5-diphenyltetrazolium bromide (MTT) was used (Singh et al. 2016a, 2016b). Fifty microliters of MTT was prepared (stock solution containing 5 mg/ml, diluted 1:5 in pre-warmed 0.15 M PBS prior to addition) and added to each well. Plates were incubated at 37 °C for 5 h. After incubation, 200 μ l of dimethyl sulfoxide (DMSO) was added to each well which results in the solubilization of the MTT formazan product and OD₄₅₀ was measured. The inhibition of biofilm was measured by calculating the metabolic activity in percentage by comparison of WT and Δ *drs2* mutant.

Phagocytosis and killing assay

THP-1 cells were grown in RPMI 1640 supplemented with 10% fetal bovine serum (FBS). To differentiate from monocyte to macrophage, the cells were treated with 15 nM phorbol myristate acetate (PMA) for 48 h and then washed three times. Cells were seeded with fresh media for 1 day to overcome the stress induction by PMA before infection. The WT and Δ *drs2* mutant *C. albicans* were grown to log phase in YPD media at 30 °C. Prior to infection, 1 ml cultures of each *Candida* strain were pelleted for 2 min, resuspended in RPMI 1640, vortexed for 2 min, and pass-through syringe (26-gauge needle) for 2–3 times. Macrophages were infected with *C. albicans* to ensure an infection ratio of 5:1 (pathogen/host) for 4 h, followed by treatment of amikacin (200 μ g/ml) to kill the cells outside the macrophage. Then, cells were washed with PBS and resuspended with RPMI supplemented with 10% FBS. After 24 h of infection, supernatant was collected. To determine the numbers of CFUs, supernatants were aspirated, and monolayers were washed gently with phosphate buffer solution (PBS) three times before being lysed with 0.5% Triton-X. The lysates were serially diluted in triplicate and plated on agar plates, and CFUs were determined as described previously (Liu et al. 2019).

Cytokine analysis

Supernatants of 24-h phagocytosed WT and Δ *drs2* mutant from the above experiment were either stored at –20 °C

or tested for levels of cytokines IL-6 and IL-10 using an enzyme-linked immunosorbent assay (ELISA) kit according to the manufacturer's (ABTS, Peprotech, USA) instructions (Liu et al. 2019; Thompson et al. 2019).

Statistical analysis

All experiments were performed in triplicates ($n = 3$). The results were reported as mean \pm standard deviation (SD) and analyzed using Student's *t* test in which $p \leq 0.05$ was considered statistically significant.

Results

Efflux pump activity is impaired in Δ *drs2* mutant

Efflux pump functionality was assessed in WT and Δ *drs2* mutant strains, by using R6G as a substrate of efflux pump transporters. We observed impaired R6G efflux in Δ *drs2* mutant in comparison with the WT strain (Fig. 1). Furthermore, we also validated our result by performing flow cytometric analysis using R6G and determined the mean fluorescence intensity (MFI) values at 0 min, 15 min, and 45 min to check the R6G accumulation (Fig. 2). The increase in MFI values in Δ *drs2* mutant with increasing time intervals demonstrates the impaired extrusion of R6G.

Ergosterol content is reduced leading to increased membrane fluidity in Δ *drs2* mutant

Further, we checked whether *Drs2p* deletion has any effect on the cell membrane by quantifying the ergosterol content in WT and Δ *drs2*. The results depicted a decrease in ergosterol content in Δ *drs2* mutant by 37% (Fig. 3). Additionally, we explored that membrane fluidity was enhanced in Δ *drs2* mutant as revealed by enhanced fluorescence of membrane permeate probe DPH as described in methods (Fig. 4).

Yeast to hyphal transition and biofilm formation is inhibited in Δ *drs2* mutant

Next, we sought to examine the effect of *Drs2p* deletion on hyphal morphogenesis using hyphae-inducing media such as SLAD (solid media), serum, and Spider (liquid media). The result demonstrates the inhibition of hyphae formation in Δ *drs2* mutant while WT cells display filamentation in all the above-tested media (Fig. 5). Further, we studied the biofilm formation in Δ *drs2*. Firstly, the qualitative visualization of biofilm was assessed using CV staining. We observed a decrease in biofilm formation in Δ *drs2* mutant in comparison with WT cells (Fig. 6a). The biofilm inhibition was then quantitatively validated by an MTT assay

Fig. 1 Effect of Drs2p deletion on R6G efflux. Efflux pump activity is estimated by measuring extracellular concentrations of R6G in *C. albicans* WT and $\Delta drs2$ mutant cells. Negative controls represent *C. albicans* de-energized cells without glucose. Mean of OD₅₂₇ ± SD of three independent sets of experiments is depicted on y-axis with respect to time (minutes) on x-axis

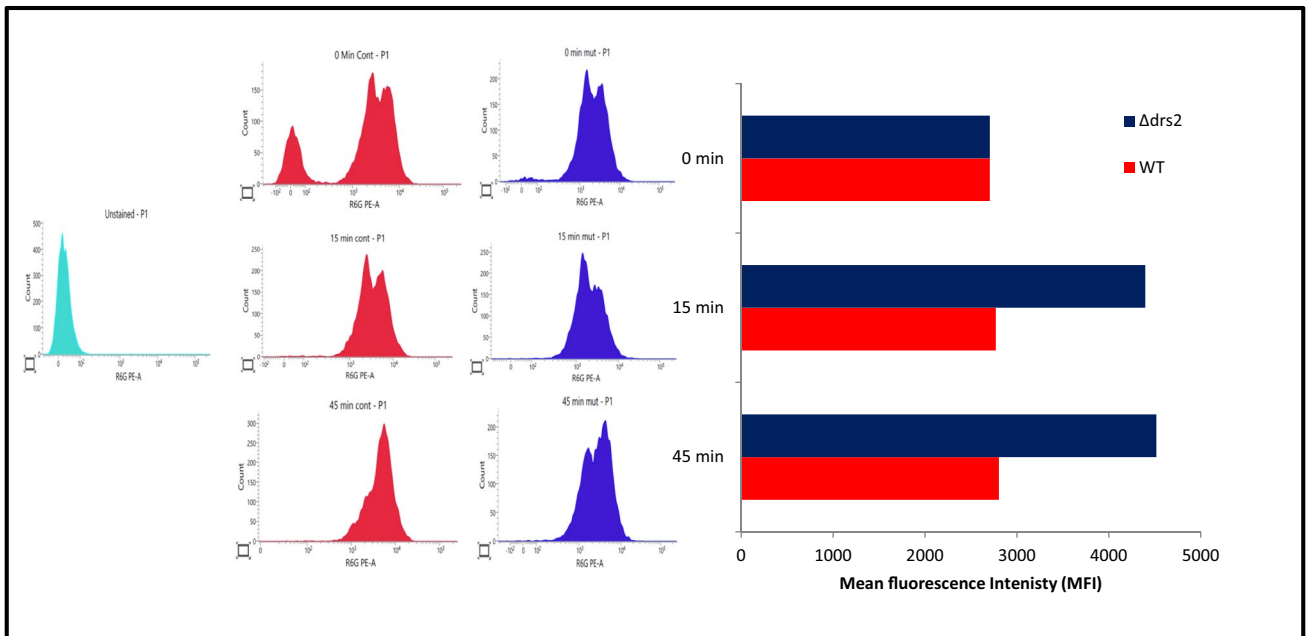
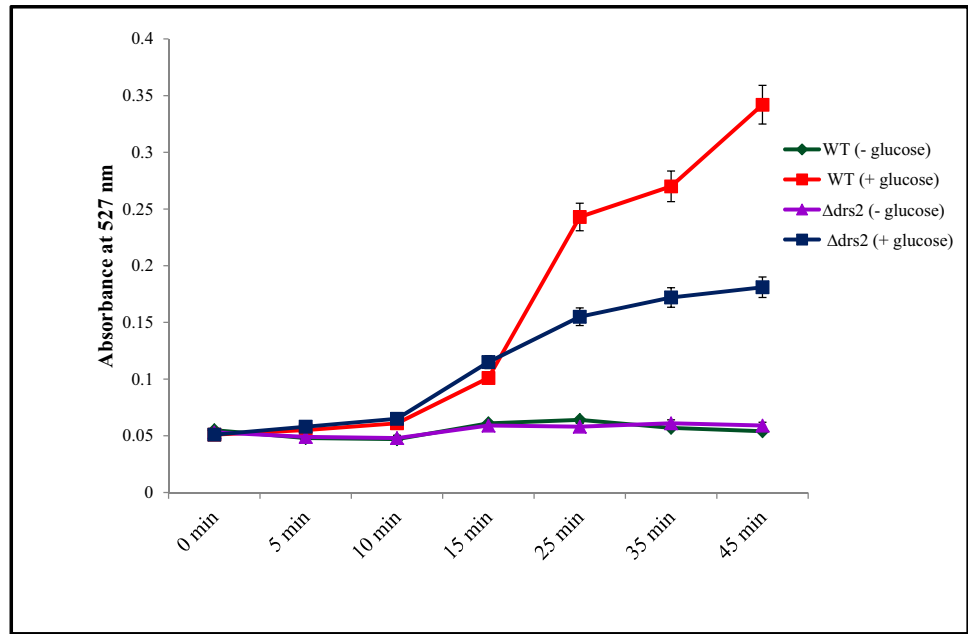


Fig. 2 Flow cytometric analysis of R6G efflux. Left panel represents histograms of WT (red) $\Delta drs2$ mutant (blue) cells stained with R6G. Green histogram represents the unstained cells as negative control.

Right panel represents MFI of R6G (10 μ M) accumulation in WT and $\Delta drs2$ mutant strains depicted at 0-min, 15-min, and 45-min time points and asterisk depicts p value < 0.05

that estimated the metabolic activity of the biofilm formation. As expected, we found reduced metabolic activity in $\Delta drs2$ mutant that confirmed impaired biofilm formation (Fig. 6b).

Macrophage killing is enhanced with $\Delta drs2$ mutant

The growth inside the macrophage of *Candida* WT and $\Delta drs2$ mutant was indirectly determined by colony-forming

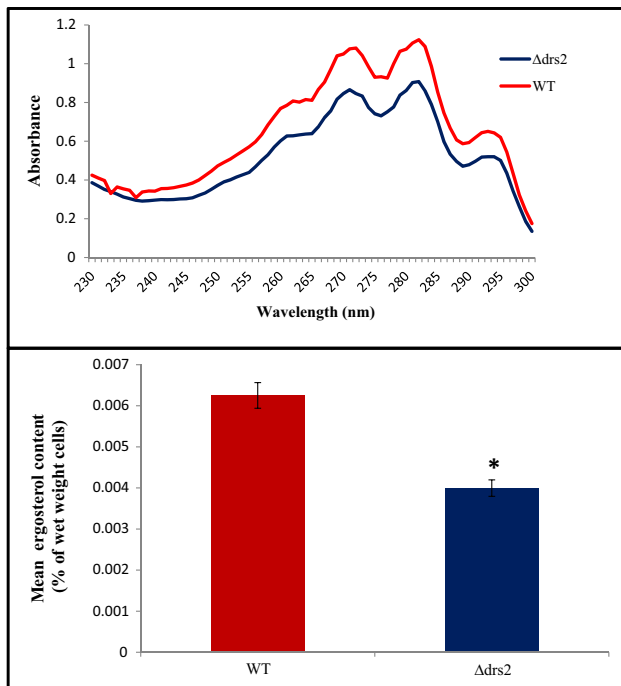
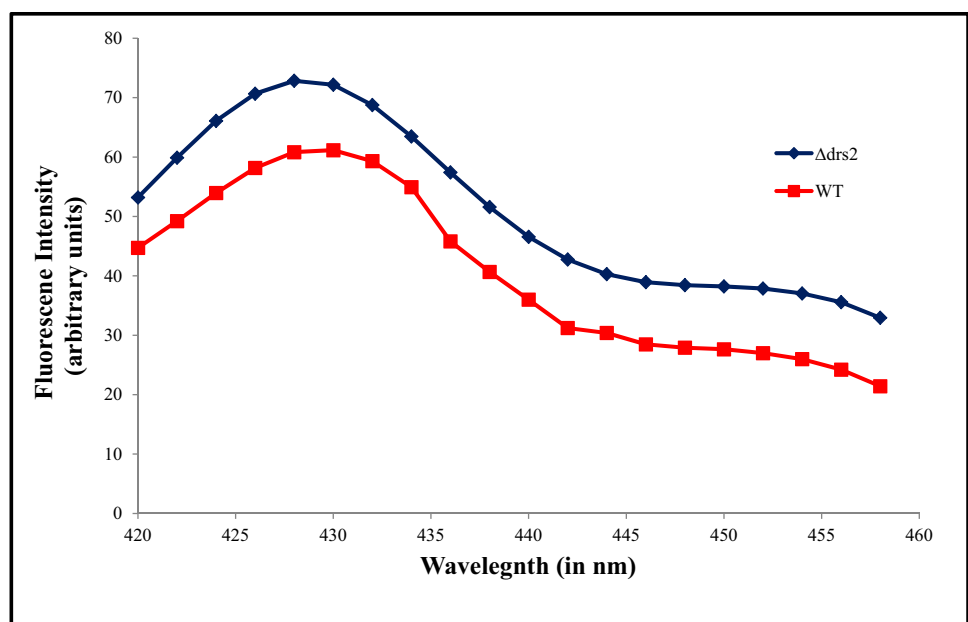


Fig. 3 Effect of Drs2p deletion on ergosterol content. Upper panel shows UV spectrophotometric ergosterol profiles of *C. albicans* WT and $\Delta drs2$ mutant cells scanned between 220 and 300 nm from overnight grown cultures. Lower panel shows relative percentages of ergosterol content in the presence WT and $\Delta drs2$ mutant. Mean of % ergosterol levels is calculated as described in “Material and methods” section normalized by considering the untreated control as $100 \pm SD$ of three independent sets of experiments is depicted on y-axis, and asterisk depicts p value < 0.05

Fig. 4 Effect of Drs2p deletion on membrane fluidity. DPH fluorescence assay to assess membrane fluidity in WT and $\Delta drs2$ mutant strains. Mean fluorescent intensity (MFI) from three independent experiments is plotted on y-axis and wavelength on x-axis



unit (CFU) to estimate the phagocytosis through macrophage killing assay. We monitored the CFU after 24-h infection and found that the infected macrophages with $\Delta drs2$ mutant showed decreased fungal growth with $79 \text{ CFU log}_{10}^5/\text{ml}$ contrary to WT depicting $125 \times \text{CFU log}_{10}^5/\text{ml}$ suggesting enhanced phagocytosis (Fig. 7).

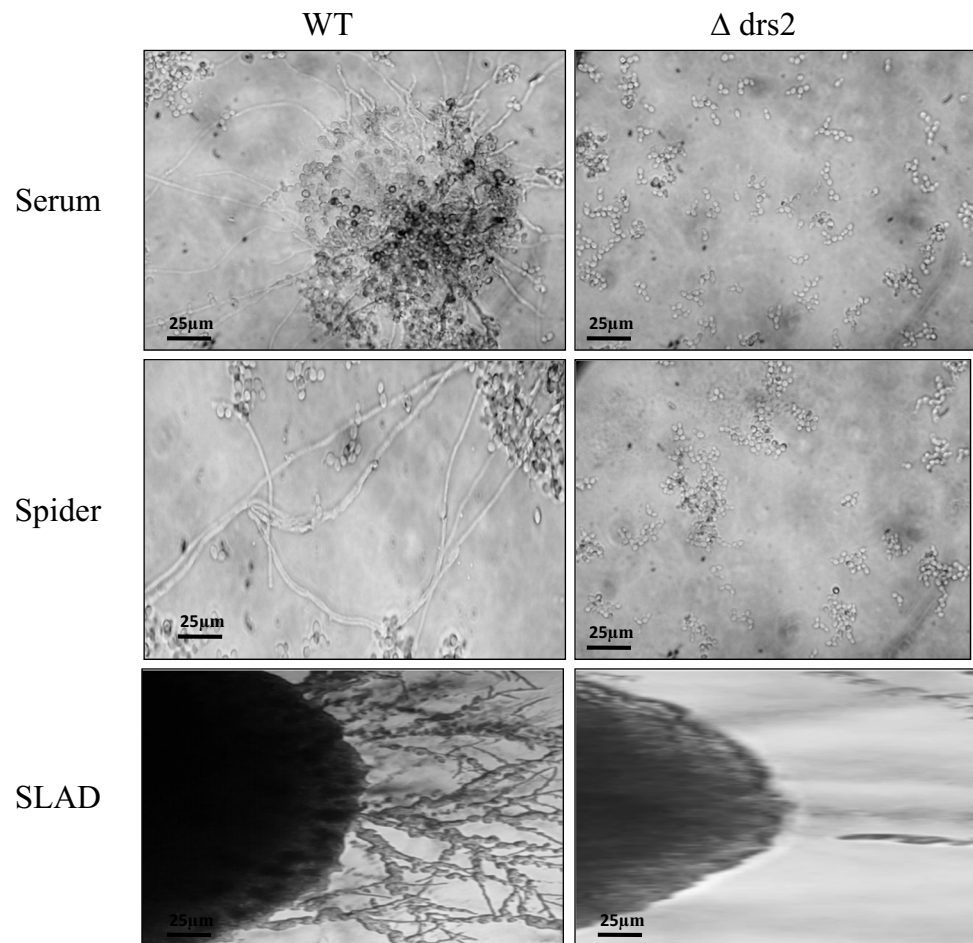
Cytokine production is altered in $\Delta drs2$ mutant

Next, we aimed to assess whether deletion of Drs2p affected the ability of *C. albicans* to stimulate cytokine production by THP-1 cell lines. We checked the level of both pro-inflammatory and anti-inflammatory cytokine secretion of THP-1 cells upon $\Delta drs2$ mutant infection. After *Candida* phagocytosis of 24 h, THP-1 cell supernatants were collected, and cytokine (IL-6 and IL-10) levels were determined by ELISA (see “Material and methods” section). We explored enhanced production of the pro-inflammatory cytokine, IL-6 (Fig. 8a), in THP-1-infected cells with $\Delta drs2$ mutant and a decrease in anti-inflammatory cytokine IL-10 levels (Fig. 8b).

Discussion

Searching for new drugs is always a viable a strategy, but it is a time-taking process and involves multiple clinical trials. The other alternative could be the identification of novel targets, which is specific for *C. albicans* such as mechanisms in ion signaling and transduction network that regulates essential pathways specific to fungal survival (Li et al. 2018). The central biosynthetic pathways in *C. albicans* can be studied for antifungal targets that help *C. albicans* to adapt its

Fig. 5 Effect of Drs2p deletion on yeast to hyphal transition. Upper panel shows hyphal morphogenesis in the liquid hyphal-inducing media (YPD with 10% serum and Spider media) in the WT and $\Delta drs2$ mutant at 4 h (magnification 40 \times). Lower panel shows hyphal morphogenesis in the solid hyphal inducing medium (SLAD) in the WT and $\Delta drs2$ mutant at 6 days (magnification 4 \times). Scale bar represents 25 μ m



metabolism for maximal virulence in host cells (Wijnants et al. 2022). P-type ATPases are a large family of ubiquitous transmembrane transporters, which are involved in the transportation of cations or metal ions across the membrane. They are divided into five classes, viz. P1 to P5, and some members of this subfamily such as the P4 type are specifically involved in the translocation of phospholipids to create membrane lipid asymmetry and thereby regulate cell division and vesicle-mediated transport in the secretory pathways (Zhou et al. 2013). There are five P4-type ATPases such as Dnf1p, Dnf2p, Dnf3p, Drs2p, and Neo1p known as lipid flippase or aminophospholipid translocase in *Saccharomyces cerevisiae* (yeast). Among them, the Drs2p forms a complex with Cdc50p, which is a non-catalytic unit. The amino phospholipids, PE, and PS are the most favorable substrates of Drs2p. Amino phospholipid transporter Drs2p localizes to the trans-Golgi network and is involved in protein and lipid transport (Natarajan et al. 2004). The present study aimed to further elucidate the role of this aminophospholipid translocase and explored the multifaceted effects of Drs2p deletion in *C. albicans*. Most strikingly, we have exposed the linkage of Drs2p deletion with major MDR mechanisms and immune recognition in *C. albicans*.

It is well established that overexpression of drug efflux pumps localized on the cell membrane is majorly responsible for MDR development in *C. albicans* (Prasad et al. 2016, 2019). Hence, R6G efflux was monitored in $\Delta drs2$, and it was confirmed that R6G efflux was impaired in $\Delta drs2$ mutant in comparison to WT (Fig. 1). This result was further validated by flow cytometry analysis which demonstrated enhanced MFI values in the case of R6G-stained $\Delta drs2$ mutant strain in comparison with WT (Fig. 2). This was indicative of the impaired activity of drug transporters in $\Delta drs2$. Additionally, we could detect some cell population at zero time point in WT which could be due to the presence of some heterogeneous cells in different morphological states or life cycle showing differential R6G accumulation but was ignored for result interpretation. Since the cell membrane is the main target of antifungal drugs such as azoles and impairment of efflux pump activity found in this study led us to observe the cell membrane more intricately. Ergosterol is a crucial component of the cell membrane in *Candida* and targets for drugs belonging to the azole class (Barrett-Bee and Dixon 1995). We found that ergosterol content was significantly reduced by 37% in $\Delta drs2$ mutant (Fig. 3). Decreased ergosterol content in $\Delta drs2$ mutant could

Fig. 6 Effect of Drs2p deletion on biofilm formation. **(a)** Crystal violet staining showing biofilm formation in the WT and $\Delta drs2$ mutant strains. **(b)** Metabolic activity of biofilm depicted as a bar graph and quantified using MTT assay. Data are expressed as mean \pm SD of three independent sets of experiments; asterisk depicts p value < 0.05

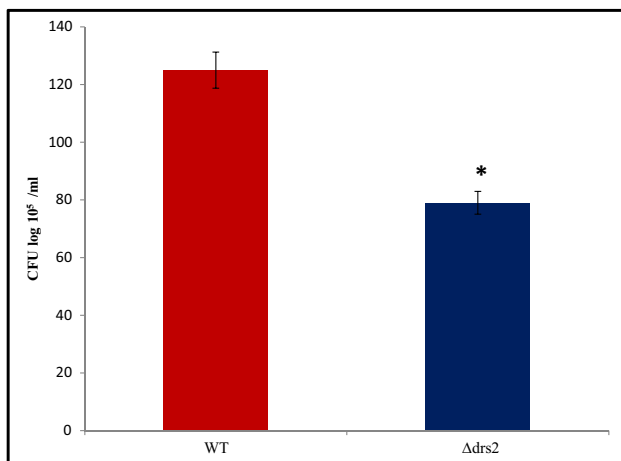
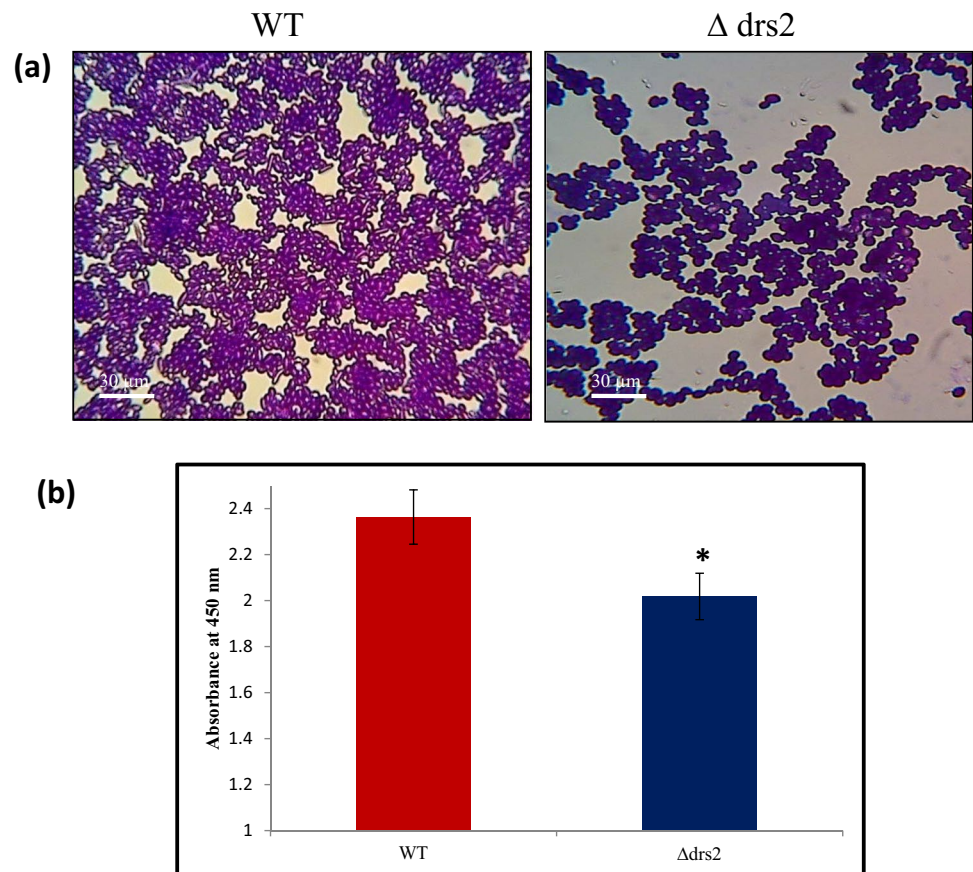


Fig. 7 Effect of Drs2p deletion on macrophage killing ability. Bar graph represents CFU log 10^5 /ml on y-axis after 24-h infection with WT and $\Delta drs2$ mutant depicting the killing of *C. albicans* by macrophages. Data are expressed as mean \pm SD of three independent sets of experiments. Asterisk depicts p value < 0.05

also explain the abrogated efflux pump activities observed above because ABC transporters are preferentially localized to membrane raft region which is rich in ergosterol (Pasrija et al. 2008). Ergosterol is also known to regulate

membrane fluidity due to its planar and rigid structure. Thus, any changes in ergosterol content could influence the membrane fluidity (Prasad et al. 2006). To our expectation, we observed enhanced membrane fluidity in $\Delta drs2$ mutant (Fig. 4) commensurate with the decreased ergosterol content observed in this study. All these results reinforce the fact that membrane homeostasis is disrupted in the $\Delta drs2$ mutant. These observations are also commensurate with the fact that $\Delta drs2$ mutant showed enhanced sensitivity towards fluconazole (Labbaoui et al. 2017).

Virulence traits such as yeast to hyphal transition and biofilm formation play a crucial role in the pathogenesis of *C. albicans*. The dimorphic nature of *C. albicans* is due to its ability for hyphal morphogenesis important for host tissue invasion. The other contributor to the development of MDR is biofilms which are highly drug-resistant structures formed by *C. albicans* and the reason behind hospital-acquired infections (Kuhn and Ghannoum 2004). Hence, we also investigated the effect of *drs2p* deletion on both virulence traits such as yeast to hyphal transition and biofilm formation. Interestingly, we found inhibited hyphal growth in $\Delta drs2$ mutant in all the tested hyphal-inducing media (Fig. 5). This result prompted us to check the effect on biofilm formation since hyphal formation is a pre-requisite for biofilm formation (Gulati

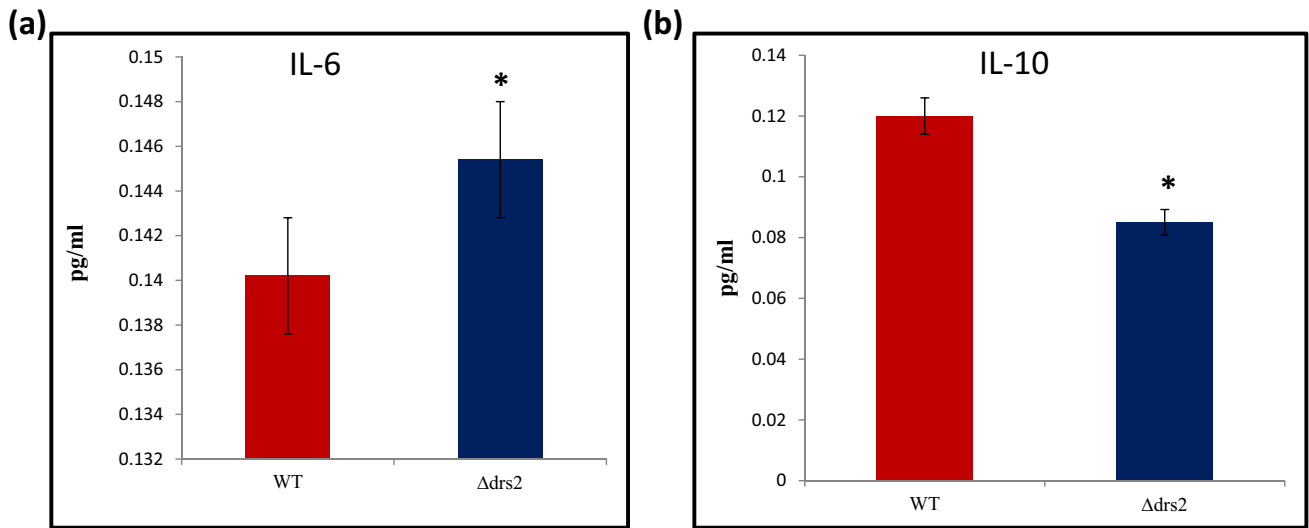


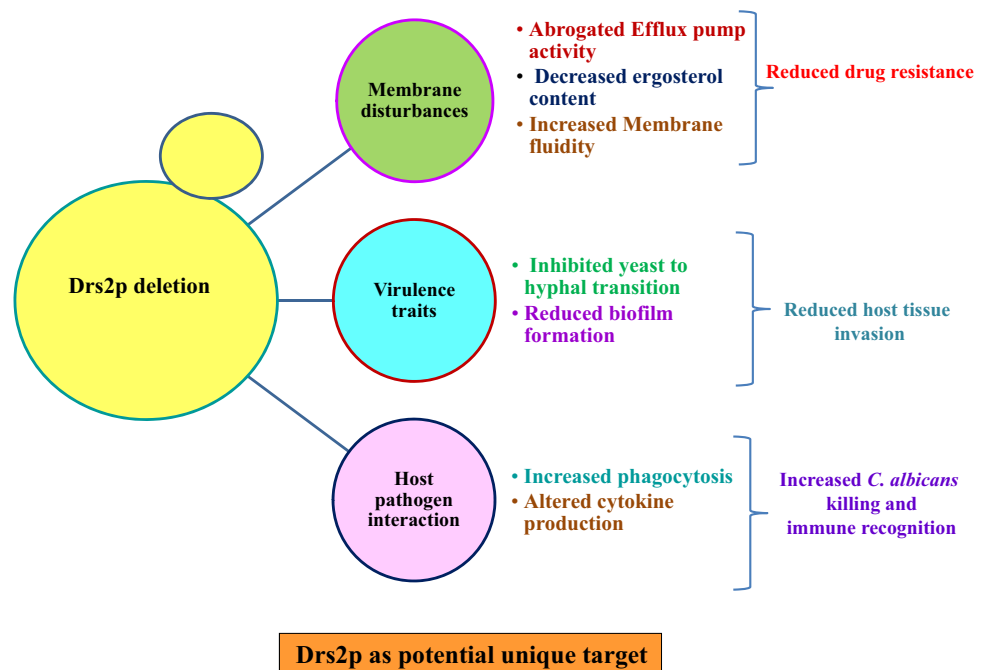
Fig. 8 Effect of Drs2p deletion on cytokine production. Bar graph represents cytokine levels measured in pg/ml on y-axis after 24-h infection with WT and $\Delta drs2$ mutant. Supernatants were collected

after infection and analyzed with specific ELISA for pro-inflammatory cytokines (a) IL-6 and (b) IL-10. The results represent the means of three independent experiments; asterisk depicts p value < 0.05

and Nobile 2016). The reduction in biofilm formation in $\Delta drs2$ mutant was evident by reduced CV staining and MTT assay depicting lower metabolic activity (Fig. 6). The biofilm formation in *C. albicans* is often attributed to the changes in the class of phospholipids and lipid raft formation levels. It is known that lipids contribute to pathogenicity, biofilm formation, drug resistance, and extracellular vesicular secretion (Rella et al. 2016). The alteration in lipid profiles could influence the cellular physiology and shape of *C. albicans*. In the early and

mature stages of biofilm formation, levels of phospholipids such as PS, PE, PC, and PA were found to be higher with respect to planktonic cells (Alim et al. 2018). The reduced biofilm formation in the present study is only fitting as it is expected that phospholipid profile will be altered in $\Delta drs2$ mutant and thereby the biofilm formation ability. The efflux pumps involved in drug resistance also coordinate in the biofilm formation as evident from the increased susceptibility of mutants of efflux pump transporters towards fluconazole in the early phase of

Fig. 9 Summary of disrupted mechanisms upon Drs2p deletion in *C. albicans*



Drs2p as potential unique target

biofilm formation (Mukherjee et al. 2003). Similarly, the link between ergosterol and biofilm formation is also demonstrated as alterations in lipid rafts influence biofilm formation (Lattif et al. 2011; Alim et al. 2018).

Lastly, in vivo studies using THP1 cell lines demonstrated how the host–pathogen interactions are affected with *C. albicans* $\Delta drs2$ mutant strain. *C. albicans* can colonize and invade tissues in the human host, exhibiting crucial mechanisms to facilitate their own survival and disseminate the infections at different niches. However, host cells also exhibit several defense mechanisms to evade the *C. albicans* infections from host tissues. One of the defense responses is induction of phagocytosis by macrophage-mediated killing and immunomodulation by the production of cytokines (Maródi et al. 1991; Káposzta et al. 1998). Macrophages represent a part of the first line of defense in immune responses and are distributed at various sites of tissues (Brunke and Hube 2013). They are important as they restrict the *C. albicans* infections and activate other immune effector cells (Krysan et al. 2014). In our study, we explored that phagocytosis is enhanced in $\Delta drs2$ mutant through macrophage killing assay as revealed by low CFU hinting its vulnerability to cause infection (Fig. 7). During phagocytosis, macrophages are known to secrete various pro- and anti-inflammatory cytokines in response to *C. albicans* infections (Jacobsen et al. 2012). The increase in production of pro-inflammatory cytokine IL-6 (Fig. 8a) demonstrates the activation of immune responses and shows the potential of host cells to control infections. On the contrary, the decrease in anti-inflammatory cytokine IL-10 (Fig. 8b) which regulates inflammation and governs a wide variety of immune responses supports the enhanced susceptibility of $\Delta drs2$ mutant by host immune cells to suppress the infection progression. The constant presence of *C. albicans* with the feeble inflammatory response is one of the biggest hurdles in the treatment of systemic fungal infections. These observations supported the credibility that deletion of aminophospholipid translocase Drs2p enhances the immune recognition of *C. albicans* and led to phagocytosis.

Conclusion

With the growing appreciation of the emerging role of lipids in MDR acquisition, the present study has projected the role of Drs2p in governing drug resistance mechanisms and immune recognition. Overall, the results depicted the significance of *C. albicans* Drs2p for functional efflux pump activity, membrane homeostasis, virulence attributes, and host–pathogen interaction (Fig. 9); however, further studies

will be needed to unravel the crosstalk if any among the disrupted traits.

Supplementary information The online version contains supplementary material available at <https://doi.org/10.1007/s10123-022-00262-9>.

Acknowledgements We acknowledge Dr. Martine Bassilana and Dr. Ramandeep Singh for the $\Delta drs2$ mutant strains and THP-1 cell lines as generous gifts, respectively. We thank Central Instrumentation Research Facility (CIRF), Amity University Haryana for facilitating us in flow cytometry and spectrofluorometer experiments.

Author contribution Aijaz Ahmad, Zeeshan Fatima, and Saif Hameed contributed to the study conception and design. Material preparation, data collection, and analysis were performed by Shweta Singh and Sandeep Hans. The first draft of the manuscript was written by Shweta Singh, and all authors commented on previous versions of the manuscript. All authors read and approved the final manuscript.

Declarations

Conflict of interest The authors declare no competing interests.

References

- Alim D, Sircaik S, Panwar SL (2018) The significance of lipids to biofilm formation in *Candida albicans*: an emerging perspective. *J Fungi (Basel)* 4:140
- Arendrup MC, Patterson TF (2017) Multidrug-resistant *Candida*: epidemiology, molecular mechanisms, and treatment. *J Infect Dis* 216:S445–S451
- Barrett-Bee K, Dixon G (1995) Ergosterol biosynthesis inhibition: a target for antifungal agents. *Acta Biochim Pol* 42:465–479
- Bongomin F, Gago S, Oladele RO, Denning DW (2017) Global and multi-national prevalence of fungal diseases-estimate precision. *J Fungi (Basel)* 3:57
- Brunke S, Hube B (2013) Two unlike cousins: *Candida albicans* and *C. glabrata* infection strategies. *Cell Microbiol* 15:701–708
- CDC. Antibiotic resistance threats in the United States, 2019. Atlanta, GA: U.S. Dep Health Hum Serv CDC; 2019
- Douglas LM, Konopka JB (2016) Plasma membrane organization promotes virulence of the human fungal pathogen *Candida albicans*. *J Microbiol* 54:178–191
- Fatima Z, Hameed S (2020) Lipidomic insight of anticandidal perillyl alcohol and sesamol induced candida membrane disruption: implications of lipid alteration, impaired fluidity and flippase activity. *Infect Disord Drug Targets* 20:784–797
- Gulati M, Nobile CJ (2016) *Candida albicans* biofilms: development, regulation, and molecular mechanisms. *Microbes Infect* 18:310–321
- Huang W, Liao G, Baker GM et al (2016) Lipid flippase subunit Cdc50 mediates drug resistance and virulence in *Cryptococcus neoformans*. *mBio* 7:e00478-16
- Jacobsen ID, Wilson D, Wächtler B, Brunke S, Naglik JR, Hube B (2012) *Candida albicans* dimorphism as a therapeutic target. *Expert Rev Anti Infect Ther* 10:85–93
- Káposzta R, Tree P, Maródi L, Gordon S (1998) Characteristics of invasive candidiasis in gamma interferon- and interleukin-4-deficient mice: role of macrophages in host defense against *Candida albicans*. *Infect Immun* 66:1708–1717

- Kohli A, Smriti MK, Rattan A, Prasad R (2002) In vitro low-level resistance to azoles in *Candida albicans* is associated with changes in membrane lipid fluidity and asymmetry. *Antimicrob Agents Chemother* 46:1046–1052
- Krysan DJ, Sutterwala FS, Wellington M (2014) Catching fire: *Candida albicans*, macrophages, and pyroptosis. *PLoS Pathog* 10:e1004139
- Kuhn DM, Ghannoum MA (2004) *Candida* biofilms: antifungal resistance and emerging therapeutic options. *Curr Opin Investig Drugs* 5:186–197
- Labbaoui H, Bogliolo S, Ghugtyal V, Solis NV, Filler SG, Arkowitz RA, Bassilana M (2017) Role of Arf GTPases in fungal morphogenesis and virulence. *PLoS Pathog* 13(2):e1006205
- Lattif AA, Mukherjee PK, Chandra J et al (2011) Lipidomics of *Candida albicans* biofilms reveals phase-dependent production of phospholipid molecular classes and role for lipid rafts in biofilm formation. *Microbiology (reading)* 157:3232–3242
- Li Y, Sun L, Lu C, Gong Y, Li M, Sun S (2018) Promising antifungal targets against *Candida albicans* based on ion homeostasis. *Front Cell Infect Microbiol* 8:286. <https://doi.org/10.3389/fcimb.2018.00286>
- Liu Y, Ou Y, Sun L et al (2019) Alcohol dehydrogenase of *Candida albicans* triggers differentiation of THP-1 cells into macrophages. *J Adv Res* 18:137–145
- Maródi L, Korchak HM, Johnston RB Jr (1991) Mechanisms of host defense against *Candida* species. I. Phagocytosis by monocytes and monocyte-derived macrophages. *J Immunol* 146:2783–2789
- Mukherjee PK, Chandra J, Kuhn DM, Ghannoum MA (2003) Mechanism of fluconazole resistance in *Candida albicans* biofilms: phase-specific role of efflux pumps and membrane sterols. *Infect Immun* 71:4333–4340
- Mukhopadhyay K, Prasad T, Saini P, Pucadyil TJ, Chattopadhyay A, Prasad R (2004) Membrane sphingolipid-ergosterol interactions are important determinants of multidrug resistance in *Candida albicans*. *Antimicrob Agents Chemother* 48:1778–1787
- Natarajan P, Wang J, Hua Z, Graham TR (2004) Drs2p-coupled aminophospholipid translocase activity in yeast Golgi membranes and relationship to in vivo function. *Proc Natl Acad Sci U S A* 101:10614–10619
- Oliveira DL, Rizzo J, Joffe LS, Godinho RM, Rodrigues ML (2013) Where do they come from and where do they go: candidates for regulating extracellular vesicle formation in fungi. *Int J Mol Sci* 14:9581–9603
- Pasrija R, Prasad T, Prasad R (2005) Membrane raft lipid constituents affect drug susceptibilities of *Candida albicans*. *Biochem Soc Trans* 33:1219–1223
- Pasrija R, Panwar SL, Prasad R (2008) Multidrug transporters CaCdr1p and CaMdr1p of *Candida albicans* display different lipid specificities: both ergosterol and sphingolipids are essential for targeting of CaCdr1p to membrane rafts. *Antimicrob Agents Chemother* 52:694–704
- Prasad T, Saini P, Gaur NA et al (2005) Functional analysis of CaIPT1, a sphingolipid biosynthetic gene involved in multidrug resistance and morphogenesis of *Candida albicans*. *Antimicrob Agents Chemother* 49:3442–3452
- Prasad T, Chandra A, Mukhopadhyay CK, Prasad R (2006) Unexpected link between iron and drug resistance of *Candida* spp.: iron depletion enhances membrane fluidity and drug diffusion, leading to drug-susceptible cells. *Antimicrob Agents Chemother* 50:3597–3606
- Prasad R, Rawal MK, Shah AH (2016) *Candida* efflux ATPases and antiporters in clinical drug resistance. *Adv Exp Med Biol* 892:351–376
- Prasad R, Nair R, Banerjee A (2019) Multidrug transporters of *Candida* species in clinical azole resistance. *Fungal Genet Biol* 132:103252
- Pristov KE, Ghannoum MA (2019) Resistance of *Candida* to azoles and echinocandins worldwide. *Clin Microbiol Infect* 25:792–798
- Ravikant Kaur T, Gupte S, Kaur M (2015) A review on emerging fungal infections and their significance. *J Bacteriol Mycol* 1:39–41
- Rella A, Farnoud AM, Del Poeta M (2016) Plasma membrane lipids and their role in fungal virulence. *Prog Lipid Res* 61:63–72
- Robbins N, Wright GD, Cowen LE (2016) Antifungal drugs: the current armamentarium and development of new agents. *Microbiol Spectr* 4:1–20
- Sebastian TT, Baldrige RD, Xu P, Graham TR (2012) Phospholipid flippases: building asymmetric membranes and transport vesicles. *Biochim Biophys Acta* 1821:1068–1077
- Singh S, Fatima Z, Hameed S (2015) Predisposing factors endorsing *Candida* infections. *Infez Med* 23:211–223
- Singh S, Fatima Z, Hameed S (2016) Citronellal-induced disruption of membrane homeostasis in *Candida albicans* and attenuation of its virulence attributes. *Rev Soc Bras Med Trop* 49:465–472
- Singh S, Fatima Z, Hameed S (2016) Insights into the mode of action of anticandidal herbal monoterpene geraniol reveal disruption of multiple MDR mechanisms and virulence attributes in *Candida albicans*. *Arch Microbiol* 198:459–472
- Singh S, Fatima Z, Ahmad K, Hameed S (2018) Fungicidal action of geraniol against *Candida albicans* is potentiated by abrogated CaCdr1p drug efflux and fluconazole synergism. *PLoS One* 13:e0203079
- Singh S, Fatima Z, Ahmad K, Hameed S (2020) Repurposing of respiratory drug theophylline against *Candida albicans*: mechanistic insights unveil alterations in membrane properties and metabolic fitness. *J Appl Microbiol* 129:860–875
- Tanwar J, Das S, Fatima Z, Hameed S (2014) Multidrug resistance: an emerging crisis. *Interdiscip Perspect Infect Dis* 2014:541340
- Thompson A, Griffiths JS, Walker L et al (2019) Dependence on Dectin-1 varies with multiple *Candida* species. *Front Microbiol* 10:1800
- Wiederhold NP (2018) The antifungal arsenal: alternative drugs and future targets. *Int J Antimicrob Agents* 51:333–339
- Wijnants S, Vreys J, Van Dijck P (2022) Interesting antifungal drug targets in the central metabolism of *Candida albicans*. *Trends in Pharmacol Sci* 43(1):69–79. <https://doi.org/10.1016/j.tips.2021.10.003>
- Wilson RB, Davis D, Mitchell AP (1999) Rapid hypothesis testing with *Candida albicans* through gene disruption with short homology regions. *J Bacteriol* 181:1868–1874
- Xu D, Zhang X, Zhang B, Zeng X, Mao H, Xu H, Jiang L, Li F (2019) The lipid flippase subunit Cdc50 is required for antifungal drug resistance, endocytosis, hyphal development and virulence in *Candida albicans*. *FEMS Yeast Res* 19:1–24
- Zarnowski R, Sanchez H, Covelli AS et al (2018) *Candida albicans* biofilm-induced vesicles confer drug resistance through matrix biogenesis. *PLoS Biol* 16:e2006872
- Zhou X, Graham TR (2009) Reconstitution of phospholipid translocase activity with purified Drs2p, a type-IV P-type ATPase from budding yeast. *Proc Natl Acad Sci U S A* 106:16586–16591

Publisher's note Springer Nature remains neutral with regard to jurisdictional claims in published maps and institutional affiliations.